El Cezeri
Journal of Science and Engineering
ISSN: 2148-3736

Research Article

Investigation Of Heat Transfer and Joule-Thomson Effect in Wells of Depleted Oil and Gas Reservoirs Used for Carbon Dioxide (CO_2) Storage

Okan Kon[1a], İsmail Caner[1b]
[1]Mechanical Engineering Department, Balıkesir University, 10145, Türkiye

ismail@balikesir.edu.tr.

DOI : 10.31202/ecjse.1642591
Received: 18.02.2025 Accepted: 03.08.2025
How to cite this article:
Okan Kon and İsmail Caner, " Investigation Of Heat Transfer and Joule-Thomson Effect in Wells of Depleted Oil and Gas Reservoirs Used for Carbon Dioxide (CO_2) Storage", El-Cezeri Journal of Science and Engineering, Vol: 12, Iss: 3, (2025), pp.(298-310).
ORCID: [a]0000-0002-5166-0258; [b]0000-0003-1232-649X

Abstract This study investigated the heat transfer mechanisms and the Joule-Thomson effect at the wellhead while storing carbon dioxide (CO_2) in depleted oil, gas, and coal reservoirs. It was assumed that the injected CO_2 for storage is in a single-phase pure state. In the reservoir well, convection heat transfer along the wellbore and conduction heat transfer with the surrounding rock soil were analysed during the production of CO_2 to the surface. Additionally, the cooling effect at the wellhead caused by the Joule-Thomson effect was examined. A positive value of the Joule-Thomson coefficient indicated the presence of a cooling effect. For the production well, the study considered temperatures of 30, 51, and 78 °C, pressures of 3.8, 4.3, and 6.1 MPa, and well depths of 1000, 1700, and 2600 meters. Six different rock-soil types surrounding the production well at the reservoir head were included, with a thermal gradient of 25 °C/km and a CO_2 flow velocity of 1 m/s. The calculated difference in conduction and convection heat loss between the wellhead entry and exit ranged from 23.918 to 481.980 W. The Joule-Thomson coefficient was found to vary between 6.797 and 17.91 0C/MPa, depending on the depth, temperature and pressure of the well. The change in exergy efficiency due to the Joule-Thomson effect (throttling exergy) was calculated to vary between 3.042 and 10.766.

Keywords: Carbon dioxide storage, Exergy analysis, Heat transfer, Joule-Thomson effect, Reservoir.

I. INTRODUCTION

The geological storage of CO_2 in reservoirs helps reduce carbon dioxide emissions and is recognized as a feasible approach in the literature. Numerous studies have demonstrated that underground oil and gas reservoirs and coal seams are suitable for the long-term storage of CO_2. Although CO_2 storage capacity is unevenly distributed worldwide, it offers the potential for storage over thousands of years [1]-[2].

The physical properties of CO_2 are crucial in determining the depth and conditions under which storage should occur. Therefore, the different phase states of CO_2 and their effects on underground storage conditions must be studied. At temperatures below the critical temperature and pressures above the vaporization curve, CO_2 exists as a liquid. However, at temperatures and pressures above the critical point, CO_2 is considered a supercritical fluid. Under supercritical conditions, a fluid exhibits properties distinct from those of either the liquid or gas phases. In underground reservoirs, both temperature and pressure increase with depth. While an increase in pressure leads to higher CO_2 density, an increase in temperature has a counteracting effect, reducing the density of CO_2 [1]-[2].

Reservoirs suitable for CO_2 storage must possess specific characteristics. They should be capable of accommodating the desired volume of CO_2, allowing for its injection at a certain rate, and preventing the leakage of light and mobile CO_2 into other subsurface regions. The reservoir must be deeper than 800 meters to achieve sufficient density through pressurisation. CO_2 injected into depths of 800 meters or more becomes a high-density fluid but remains lighter than water. Above this depth, CO_2 exists as a gas with a low density for economically viable storage [1]-[2].

Currently, 18 large-scale commercial carbon capture and storage (CCS) projects are operational, with a total annual CO_2 capture capacity of approximately 40 million tons. To date, 230 million tons of CO_2 have been safely injected underground. This practice is predominantly concentrated in countries like the United States, China, Canada, Australia, and Norway, where oil recovery and coal production are widespread [1]-[2].

A comprehensive review of the literature reveals key insights from various researchers. Abass A. Olajire [3] examined predictive models for gas hydrate formation in gas flow cycles, focusing on management strategies such as chemical injection and pressure reduction to mitigate hydrate risks. He emphasized that these methods help ensure safe production and prevent

economic losses. Li et al. [4] investigated CO_2 injection in the Weyburn Midale cap rock, concluding that CO_2 leakage occurs through volume flow and emphasizing the importance of sealing pressure for preventing leakage. They also found that increasing reservoir pressure does not significantly boost storage capacity, but removing water from the reservoir could enhance it. Manovic et al. [5] explored CO_2 storage concepts, outlining criteria for site selection and long-term monitoring as key challenges. Liu et al. [6] discussed waste heat recovery from mature oil and gas reservoirs, proposing a framework for assessing low-temperature recovery potential. Their study on the Villafortuna-Trecate oil field demonstrated that a single well could recover about 25 GWh of electricity over 10 years. Yan et al. [7] analysed deep-borehole heat exchangers for geothermal systems, showing that irregular insulation improves cooling efficiency, achieving up to 21.8% energy savings. Wang et al. [8] proposed a hydro-thermal model for shale oil production, showing that increasing temperature by 60 K could boost production by 31.16% and emphasizing the importance of formation factors. Guo et al. [9] proposed a semi-analytic solution for groundwater flow in geothermal heat pumps, achieving high computational efficiency while maintaining accuracy. Bai et al. [10] addressed well integrity in CO_2 sequestration, focusing on corrosion issues and proposing new risk-based evaluation methods. Amar et al. [11] developed AI models for predicting CO_2 thermal conductivity, outperforming traditional methods. Liu et al. [12] highlighted the potential of closed-loop heat extraction systems in abandoned wells and stressed the need for further optimization. Jia et al. [13] demonstrated that a smooth velocity profile reduces friction in CO_2 flow, suggesting adjustments to minimize friction losses. Zhou et al. [14] examined advanced thermal techniques in abandoned wells, emphasizing renewable integration and carbon neutrality strategies. Kengerli and Agayeva [15] modelled the impact of integrating a new gas pipeline, observing initial instability before system equilibrium. Apak [16] developed an analytical model for drilling fluid temperatures, validated with simulations. Sorgun [17] explored drilling fluids and cutting transport in inclined wells, finding that fluid velocity and pipe rotation significantly affect performance. Ettehadi [18] assessed sepiolite-based mud under challenging conditions, noting temperature effects on viscosity. Ahmed et al. [19] analysed heat exchangers in geothermal systems, showing that well length impacts heat transfer rates and pressure drop.

Holloway [20] explored CO_2 capture and geological storage technologies, focusing on the processes involved in capturing CO_2 at industrial sites, transporting it to storage locations, and ensuring its long-term containment. He identified cost and financing issues related to underground storage as key challenges. This technology is gaining traction due to the continued dependence on fossil fuels for energy production. Bachu [21] proposed 15 criteria for evaluating sedimentary basins for CO_2 sequestration, stressing that warm basins are less suitable due to higher CO_2 rise tendencies and lower storage capacities. His method calculates suitability scores, offering flexibility by adjusting the importance of each criterion, and it was applied to Canadian and Alberta basins. Bahadori and Vuthaluru [22] created a tool to predict CO_2's transport properties, such as viscosity and thermal conductivity, with fewer parameters than existing models. Their tool showed an average deviation of 1.1% for viscosity and 1.3% for thermal conductivity, providing a practical approach for engineers and regulators. Vesovic et al. [23] introduced new CO_2 viscosity and thermal conductivity equations, based on experimental data and theoretical models. These equations are valid for temperatures between 200 K and 1500 K and pressures up to 100 MPa, offering accurate predictions with small uncertainties.

Pipelines, initially constructed in the late 1800s for transporting low-calorific coal gas, are now the primary means of transporting gas. The capacity of pipelines is mainly determined by operating pressure and diameter, with increasing diameters up to 48 inches, which may mark the practical limit for land-based pipelines. Increasing operating pressures is a more common solution to meet growing demand than expanding diameters. Most transmission pipelines operate at pressures above 60 bar, with some reaching 125 bar, requiring larger pipes, bigger compressors, and more stringent safety standards, leading to higher costs [24]. CO_2 is widely used in Enhanced Oil Recovery (EOR), which helps release trapped oil, and CO_2 injection projects produce thousands of barrels daily. CO_2 is also an effective long-term storage method for CO_2 sequestration when available at low costs [25].

A model for high-temperature, high-pressure wells was validated using data from a gas well in China, showing accurate gas pressure and temperature predictions along the well's depth, with implications for dynamic production analysis [26]. Extracting geothermal energy from abandoned oil wells offers an opportunity to extend their life, but technical, economic, and regulatory factors must be addressed. A comprehensive review provides insights into these challenges and the policies for converting these wells into geothermal energy sources [27]. A roadmap for evaluating low-temperature waste heat recovery from mature oil and gas reservoirs was tested in Italy, showing that a single well could generate 25 GWh of electrical energy over a decade [6]. The use of computational fluid dynamics and equations of state to predict the Joule-Thomson (JT) effect in gases was validated with industrial natural gas data, highlighting its importance in industrial applications [28]. Modern drilling often shows variations between well fluid temperatures and the original reservoir temperature, significantly affecting low-permeability reservoirs and high-pressure conditions. An analytical model was developed to predict fluid temperature distribution, accounting for the Joule-Thomson effect, and validated with field data, enabling more accurate predictions of parameters like the productivity index [29]. A study on single-phase oil reservoirs developed a 1D radial flow model to predict fluid temperature changes, showing how production rate impacts reservoir heating and fluid properties. The model is also applicable to single-phase gas reservoirs [30]. Micro-scale thermal effects during ultra-deep gas well production were accounted for in a model predicting bottom-hole temperature changes, showing that factors like gas production rate and initial formation conditions affect flow temperature [31]. CO_2 Plume Geothermal systems outperform traditional geothermal systems

at low temperatures. This study explores heat transfer within the wellbore in CO_2-based geothermal operations, suggesting that the wellbore flow can remain adiabatic during much of the system's lifespan [32]. CO_2 storage in depleted gas reservoirs is feasible, providing secure long-term storage, with capacity dependent on various factors [33]. The Joule-Thomson effect's importance in mechanical engineering and its thermodynamic properties were analysed, alongside the throttling effect of gases on pressure, temperature, and flow rate [34]-[35]. Using CO_2 as a heat transfer fluid in geothermal systems shows higher heat extraction rates than water-based systems, allowing more regions to generate geothermal electricity while ensuring CO_2 storage for negative carbon emissions [36].

The primary objective of this study is to analyse the heat transfer mechanisms involved in the storage of CO_2 in depleted hydrocarbon reservoirs at power plants, specifically focusing on the calculation of the Joule-Thomson (JT) coefficient at the wellhead ve well bottom. The research aims to explore various operational conditions, considering three distinct temperatures (30°C, 51°C, and 78°C), three different pressures (3.8 MPa, 4.3 MPa, and 6.1 MPa), and three well depths (1000 m, 1700 m, and 2600 m). Furthermore, the study examines various rock types, including sandy subclay, sand, sandstone, conglomerate, andesite, and gneiss, considering their respective properties, such as specific heat capacity, thermal conductivity, and thermal diffusivity. The physical exergy and exergy efficiency changes of the Joule-Thomson effect (throttling exergy) at the atmospheric outlet were calculated based on the pressure and temperature of CO2 at the wellhead and well bottom. The exergy heat loss was determined for both conduction and convection heat losses at the reservoir outlet.

Joule-Thomson effect (throttling process): It refers to the process in which a gaseous fluid flows from a high-pressure environment to a lower-pressure environment through a narrow opening. This narrow opening can be equipment such as a nozzle, valve, or orifice. During this process, no work is done externally, the pressure of the gas decreases, and its temperature changes. The temperature change may increase or decrease depending on the type of gas. For carbon dioxide in this study, the pressure decreases [35].

In the study, a well thermal gradient of 25°C/km, a CO_2 flow velocity of 1 m/s, and an ambient temperature of 5°C were selected. The rock and soil porosity were set at 0.1, and the well diameter was fixed at 0.100 m. By examining these parameters, the research aims to provide a comprehensive understanding of the thermal behaviour of CO_2 under varying conditions, contributing to the optimization of CO_2 storage processes in depleted reservoirs. The well depths at the reservoir outlet were taken as 1000, 1700, and 2600 meters. These depths were chosen because the pressure and temperature at the well outlet correspond to conditions where carbon dioxide remains in the gas phase. The study investigates the heat transfer mechanisms in the well, energy loss due to heat, and the Joule-Thomson effect (throttling) at the outlet following the storage of large amounts of carbon dioxide in depleted oil, gas, and coal reservoirs. In the existing literature, each of these aspects has been examined separately. However, the distinctive feature of this study is that all of these investigations are conducted together. By performing these combined analyses, the study aims to contribute to the literature.

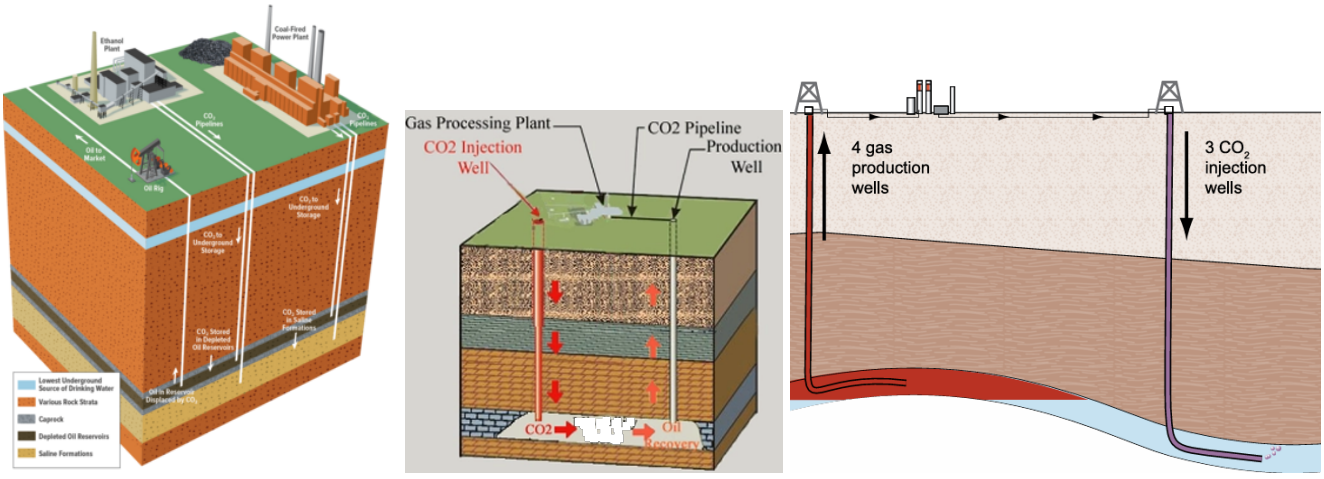

Figure 1. Transportation of carbon dioxide (CO_2) and its storage in reservoirs through wells [1]-[37]-[38].

Table 1. Storage capacity for geological storage [1]

Reservoir Type	Lower estimate of storage capacity ($GtCO_2$)	Upper estimate of storage capacity ($GtCO_2$)
Oil and Gas fields	675	900
Unmineable coal seams	3-15	200
Deep saline formations	1000	possibly 10^4

The mechanisms and equipment for transporting and storing CO_2 from power plants into reservoirs via wells are shown in Figure 1. Figure 2 illustrates suitable saline formations, oil, gas fields, and coal or coal beds where CO_2 can be stored. Table 1 presents the lower and upper storage capacities for geological storage, depending on the reservoir type worldwide.

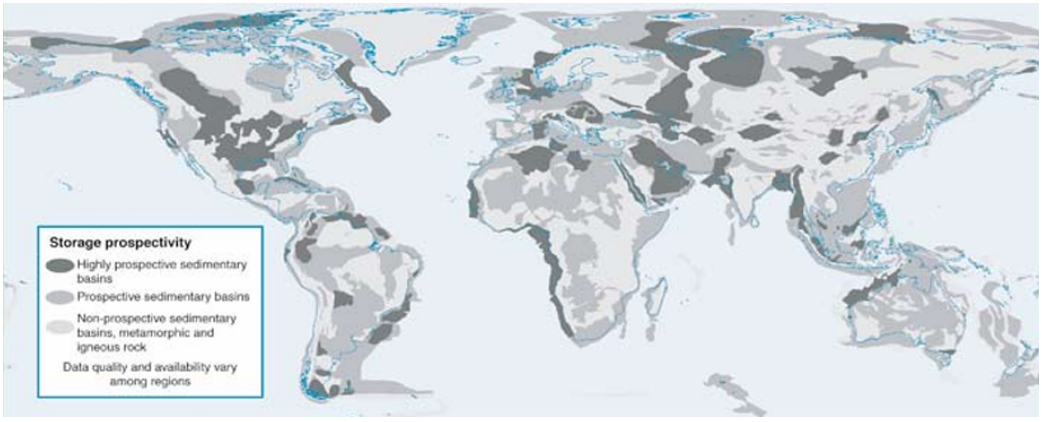

Figure 2. Worldwide Suitable saline formations, oil and gas fields, coal or coal seams where carbon dioxide (CO_2) can be stored [1].

Figure 3 presents the injection and production mechanisms in wells where CO_2 is stored in reservoirs. Figure 4 shows the heat transfer mechanisms in wells where CO_2 is stored. Figure 5 provides the wellhead equipment used for CO_2 storage. Figure 6 depicts the Pressure-Temperature diagram and phase properties for CO_2 storage.

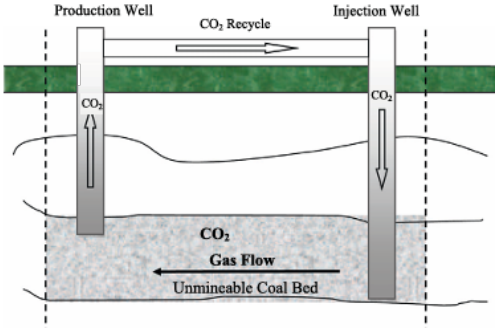

Figure 3. Injection and production well mechanisms for the storage of carbon dioxide (CO_2) [39].

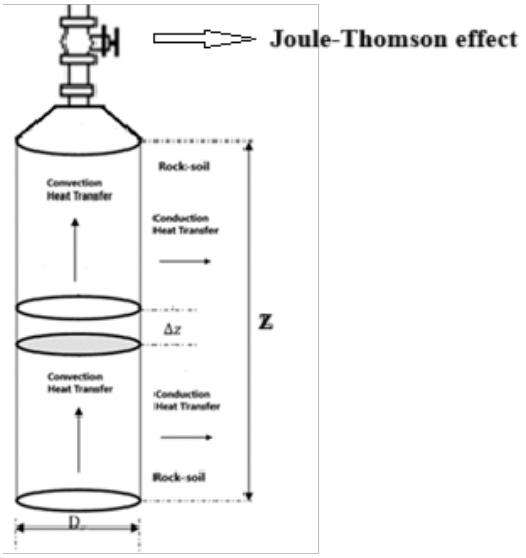

Figure 4. Heat transfer mechanisms in wells where carbon dioxide (CO_2) is stored [32]-[40].

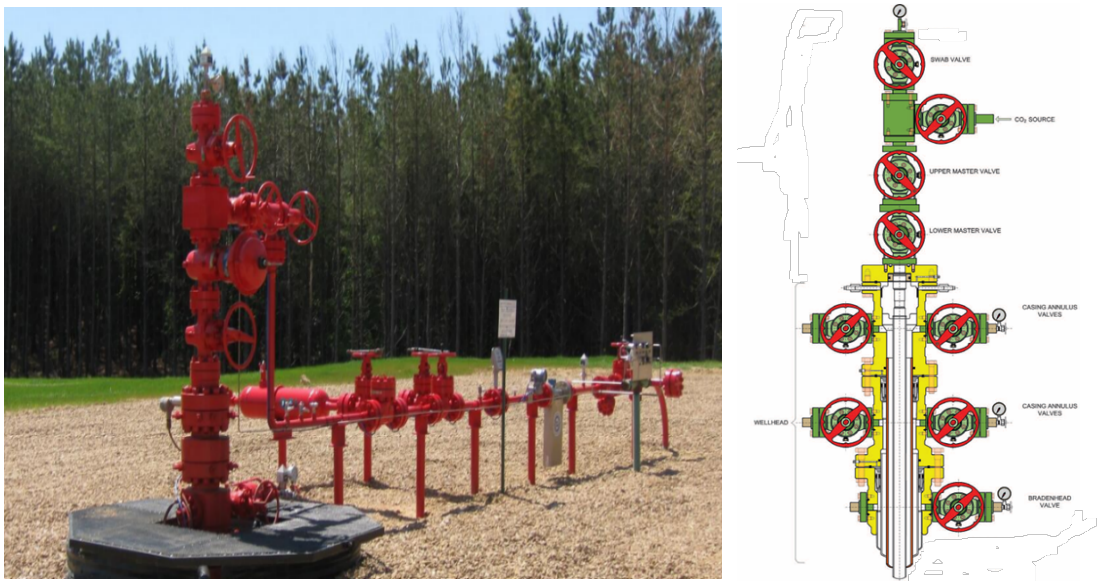

Figure 5. Wellhead equipment for storing carbon dioxide (CO_2) [41]-[42].

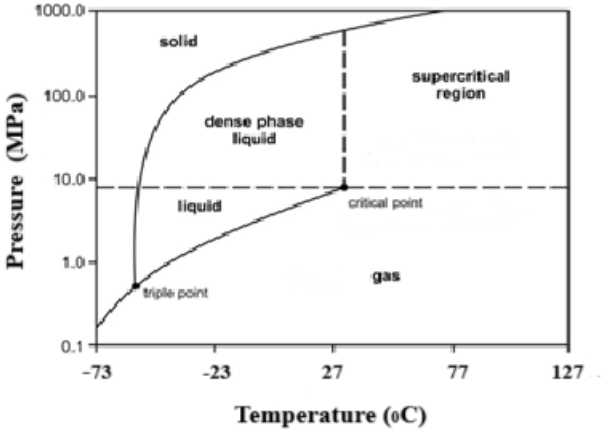

Figure 6. Pressure-Temperature diagram and phase properties for carbon dioxide (CO_2) storage [1]-[43]

II. MATERIALS AND METHOD

The values for Reservoir Temperature, Reservoir Pressure, Ambient Temperature, Thermal Gradient, Flow Velocity, Well Depth, and Well Diameter are provided in Table 2. Table 3 presents the specific heat capacity, thermal conductivity, and thermal diffusivity values for six rock-soil types: Sandy Subclay, Sand, Sandstone, Conglomerate, Andesite, and Gneiss. The critical properties of carbon dioxide, including its critical temperature, critical pressure, and critical density, are shown in Table 4. Equations (1–6) are used to calculate the thermal conductivity and viscosity of carbon dioxide (CO_2). The correlation used to determine the thermal conductivity and viscosity of carbon dioxide is a function of pressure. The four coefficients in the equation (a, b, c, d) depend on the properties of CO_2 within the temperature range of -13 to 177 °C and the pressure range of 10–70 MPa [22]. Equations (7) and (8) are used to determine the Joule-Thomson coefficient at the wellhead based on temperature and pressure differences. The Joule-Thomson coefficient at the reservoir well outlet represents the temperature change per unit pressure change.

$$\ln \lambda = a + \frac{b}{P} + \frac{c}{P^2} + \frac{d}{P^3} \quad (1)$$

$$\ln \mu = a + \frac{b}{P} + \frac{c}{P^2} + \frac{d}{P^3} \quad (2)$$

$$a = A_1 + \frac{B_1}{T} + \frac{C_1}{T^2} + \frac{D_1}{T^3} \quad (3)$$

$$b=A_2+\frac{B_2}{T}+\frac{C_2}{T^2}+\frac{D_2}{T^3} \quad (4)$$

$$c=A_3+\frac{B_3}{T}+\frac{C_3}{T^2}+\frac{D_3}{T^3} \quad (5)$$

$$d=A_4+\frac{B_4}{T}+\frac{C_4}{T^2}+\frac{D_4}{T^3} \quad (6)$$

Table 2. Parameters and Values Used for Calculations in the Study [32]-[44]-[45]-[46].

Parameter	Value
Reservoir Temperature	30, 51, 78 ^{0}C
Reservoir Pressure	3.8, 4.3, 6.1 MPa
Ambient Temperature	5 ^{0}C
Thermal Gradient	25 ^{0}C/km
CO_2 flow velocity	1 m/s
Rock and Soil Porosity	0.1
Well Depth	1000, 1700, 2600 m
Well Diameter	0.100 m
Well Roughness	0.000045 m

Table 3. Rock-Soil Properties and their [47]-[48].

Rock-Soil Thermal Conductivity	Specific Heat Capacity (kJ/kg.K)	Thermal Conductivity (W/m.K)	Thermal Diffusivity (mm2/s)
Sandy Subclay	1.289	1.738	0.681
Sand	1.079	1.989	0.955
Sandstone	0.789	1.967	1.035
Conglomerate	0.795	1.726	0.916
Andesite	0.785	2.084	1.062
Gneiss	0.782	2.553	1.231

Table 4. Critical Properties of Carbon Dioxide (CO2) [1].

Parameter	Value
Molecular Weight	44.01 kg/kmol
Critical Temperature	31 ^{0}C
Critical Pressure	7.39 MPa
Critical Density	467.7 kg/m^3

Table 5. Coefficients for the Calculation of Thermal Conductivity and Viscosity of Carbon Dioxide (CO2) [22]

	Thermal Conductivity (λ_f)	Dynamic Viscosity (μ_f)	
Symbol	Coefficients for thermal conductivity of carbon dioxide	Coefficients for viscosity of carbon dioxide at temperatures less than 67 ^{0}C	Coefficients for viscosity of carbon dioxide, at temperature more than 67 ^{0}C
A_1	2.511772164091	-8.381727231932328 x 10^1	-6.304360942940384 x 10^1
B_1	-4.61299395833 x 10^3	7.170262916398216 x 10^4	7.089412819202834 x 10^4
C_1	1.56039978824 x 10^6	-2.077352606491789 x 10^7	-2.729618206187531 x 10^7
D_1	-1.6486817476956 x 10^8	2.035238087953347 x 10^9	3.491954145885637 x 10^9
A_2	-6.7843586693162 x 10^2	7.688274861237018 x 10^3	5.392507286567643 x 10^3
B_2	5.9472900533367 x 10^5	-6.832908603727831 x 10^6	-6.48675327864201 x 10^6
C_2	-1.8136903173662 x 10^8	2.00319868619153 x 10^9	2.543938513422521 x 10^9
D_2	1.8606361834906 x 10^{10}	-1.94536522596535 x 10^{11}	-3.281228975928387 x 10^{11}
A_3	2.0648978571659 x 10^4	-1.967260059076993 x 10^5	-1.182481836340281 x 10^5
B_3	-1.9966713570538 x 10^7	1.732142393454871 x 10^8	1.438608962538429 x 10^8
C_3	6.4236725264301 x 10^9	-5.049067845006425 x 10^{10}	-5.738803284656972 x 10^{10}
D_3	-6.8021988393284 x 10^{11}	4.882358762211981 x 10^{12}	7.535042772730154 x 10^{12}
A_4	-1.095035226623 x 10^5	1.3529778432466 x 10^6	6.947087585578619 x 10^6
B_4	1.0878297025052 x 10^8	-1.19567721576674 x 10^9	-8.506349304338924 x 10^9
C_4	-3.575489373317 x 10^{10}	3.498814034450212 x 10^{11}	3.424312685872325 x 10^{11}
D_4	3.8549993712053 x 10^{12}	-3.395109635057981 x 10^{13}	-4.542379235870166 x 10^{13}

Equation of Joule-Thomson coefficient [28, 29]-[34]-[35]-[37]-[38]-[55];

$$K_{JT}=\left(\frac{\Delta T}{\Delta P}\right)_{h_{en}}=\left(\frac{T_{in}-T_0}{P_{in}-P_0}\right)_{h_{en}} \tag{7}$$

$$\mu_{JT}=\left(\frac{\partial T}{\partial P}\right)_{h_{en}} \tag{8}$$

The pressure of well Van Der Waals equation can be calculated by using below equations [28, 29, 55, 57-59];

$$P_{in}=\frac{RT}{V-x}-\frac{y}{V^2} \tag{9}$$

$$x=\frac{27}{64}\frac{R^2T_c^2}{P_c^2} \tag{10}$$

$$y=\frac{RT_c}{8P_c} \tag{11}$$

The energy balance related to the heat loss of carbon dioxide (CO_2) inside the production well of a reservoir where CO_2 is geologically stored includes heat loss through conduction from the CO_2 within the well and conductive heat loss between the well and the surrounding rock-soil formations [32], [49], [50], [51], [52], [53]. The coefficients A, B, C, and D used in Equations (3–6) for the calculation of the thermal conductivity and viscosity of carbon dioxide are provided in Table 5.

Heat loss in the well during the discharge of carbon dioxide from the reservoir [33,54-55],

$$q_{storage}=q_{in\text{-}convection}-q_{out\text{-}conduction} \tag{12}$$

The equation for convection heat loss is;

$$q_{convection}=h.\,A\,.\,\Delta T \tag{13}$$

Conduction heat transfer equation is,

$$q_{conduction}=\frac{2\pi\,.\,\lambda_{rock\text{-}soil}.z.\Delta T}{\ln\left(\frac{4.Z}{D}\right)} \tag{14}$$

A is the contact area for heat transfer between carbon dioxide (CO_2) and rock-soil. h is the convective heat transfer coefficient, $\lambda_{rock\text{-}soil}$ is the heat conduction coefficient of rock-soil, z is the dept of well, and in (4.Z/D) represents the shape factor for the well. The Nusselt number is used for calculating the convective heat transfer coefficient, where D is the well diameter and λ_f is the thermal conductivity of the fluid (CO_2).

$$h=\frac{Nu\,.\,\lambda_f}{D} \tag{15}$$

For turbulent pipe, flow is used to calculate the Nusselt number (Nu) based on the Reynold number (Re) and Prandtl number (Pr).

$$Nu=0.023\,.\,Re^{0.8}.Pr^{0.4} \tag{16}$$

The Reynold number are,

$$Re=\frac{\rho.V.D}{\mu} \tag{17}$$

where ρ is density, μ is dynamic viscosity and V is the speed of carbon dioxide (CO2) [33,54-55].

General exergy equations is given below. Here T_0 is environmental temperature. T_{in} is inner side of well temperature, h_{en} is enthalpy (kJ/kg) and s_{en} is entropy (kJ/kg.K) [43]-[44]-[55];

$$E_x=h_{en}-h_{en0}-T_0(s_{en}-s_{en0}) \tag{18}$$

The exergy loss equation based on the temperature difference is given below.

$$E_x=q\,.\,\left(1-\frac{T_0}{T_{in}}\right) \tag{19}$$

Joule-Thompson effect on exergy ratio equation [43]-[44]-[55];

$$E_x=T_0\,.\,(s_{en1}-s_{en2}) \tag{20}$$

$$\varepsilon=\frac{\text{Exergy ratio before the Joule-Thompson effect}}{\text{Exergy ratio after the Joule-Thompson effect}} \tag{21}$$

III. RESULTS AND DISCUSSIONS

A Carbon dioxide (CO_2) values for different rock-soil types such as Sandy Subclay, Sand, Sandstone, Conglomerate, Andesite, and Gneiss, the heat loss by conduction for well depths of 1000 m and a well-bottom temperature of 30°C ranges from 73,460 to 108,660, and for 78°C, it ranges from 214,500 to 317,280. For a well depth of 1700 m and a well-bottom temperature of 30°C, the heat loss ranges from 124,880 to 184,720, and for 78°C, it ranges from 364,650 to 539,370. For a well depth of 2600 m and a well-bottom temperature of 30°C, the heat loss ranges from 191,000 to 282,510, and for 78°C, it ranges from 557,700 to 824,920.

The convection heat loss for Carbon dioxide (CO_2) in a well depth of 1000 m and well-bottom temperatures of 30°C and 78°C ranges from 49,542 to 132,140. A well depth of 1700 m and the same well-bottom temperatures ranges from 83,670 to 223,160; for a well depth of 2600 m, it ranges from 128,570 to 342,940.

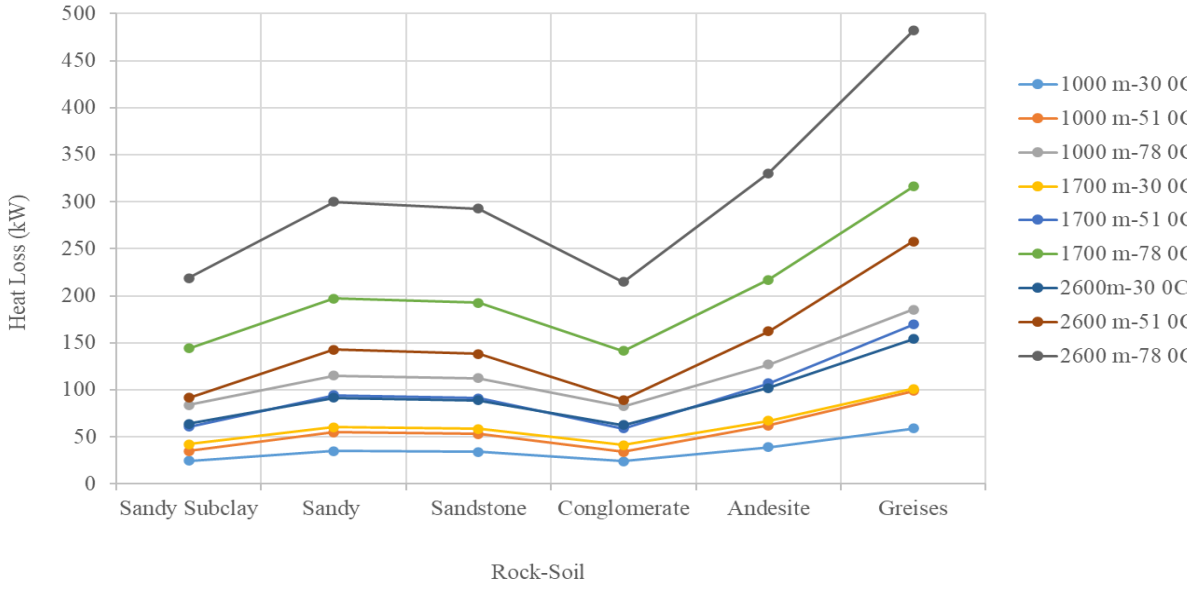

Figure 7. Heat Loss depending on rock-soil type and temperature.

Carbon dioxide (CO_2) values for a well depth of 1000 m and a well-bottom temperature of 30°C, the conduction heat loss ranges from 23,918 to 59,118, and for 78°C, it ranges from 82,360 to 185,140. For a well depth of 1700 m and a well-bottom

temperature of 30°C, it ranges from 41,210 to 101,050, and for 78°C, it ranges from 141,490 to 316,210. For a well depth of 2600 m and a well-bottom temperature of 30°C, the conduction heat loss ranges from 62,430 to 153,940, and for 78°C, it ranges from 214,760 to 481,980. A difference between conduction and convection heat loss was detected. For a well-bottom temperature of 51°C, different the heat loss for a well depth of 1000 m ranges from 34,159 to 98,909; for 1700 m, it ranges from 59,190 to 169,290; and for 2600 m, it ranges from 89,280 to 257,660. These and all other values are shown in Figure 7, with heat loss values dependent on rock-soil type, well depth, and well-bottom temperature.

For different rock-soil types such as Sandy Subclay, Sand, Sandstone, Conglomerate, Andesite, and Gneiss, the exergy heat loss for well depths of 1000 m and a well-bottom temperature of 30°C ranges from 1.972 to 4.875, temperature of 51°C ranges from 4.847 to 14.036 and for 78°C, it ranges from 17.122 to 38.488. For a well depth of 1700 m and a well-bottom temperature of 30°C, the exergy heat loss ranges from 3.398 to 8.333, for a temperature of 51°C ranges from 8.400 to 24.024 and for 78°C, it ranges from 29.414 to 65.736. For a well depth of 2600 m and a well-bottom temperature of 30°C, the exergy heat loss ranges from 5.148 to 12.695, and temperature of 51°C ranges from 12.670 to 36.564 for 78°C, it ranges from 44.646 to 100.198. These values are given in Figure 8.

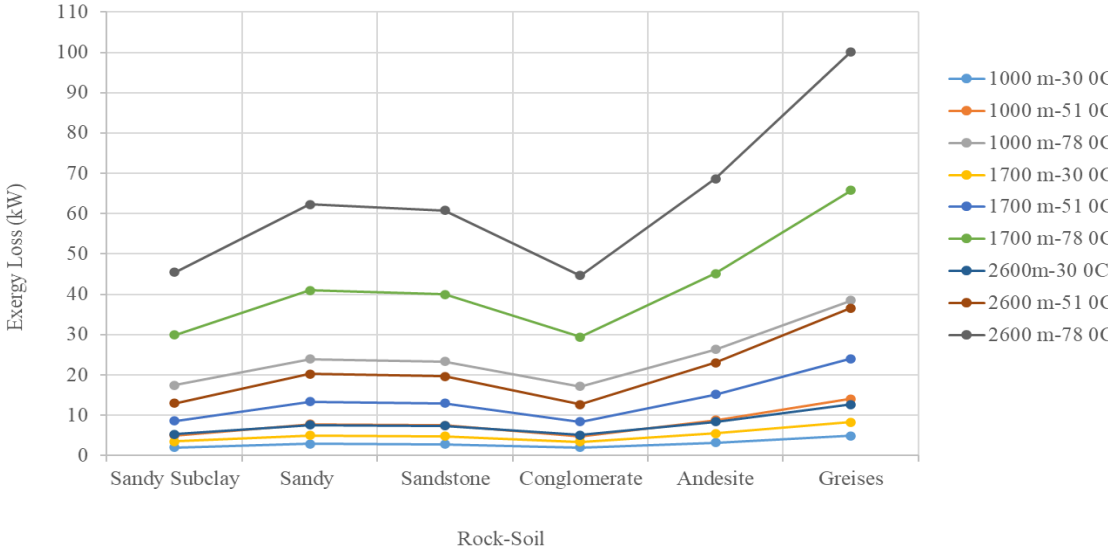

Figure 8. Exergy Loss values depending on rock-soil type and temperature.

The Joule-Thomson coefficient values for carbon dioxide (CO_2) were calculated as 7.006, 7.922, and 17.91^{0}C/MPa for 1000 m at 30 °C, 51 °C, and 78 °C, respectively; 6.866, 7.817, and 17.541 ^{o}C/MPa for 1700 m at 30 °C, 51 °C, and 78 °C, respectively; and 6.797, 7.766, and 17.365 ^{0}C/MPa for 2600 m at 30 °C, 51 °C, and 78 °C, respectively. These values are illustrated in Figure 9. These Joule-Thomson coefficient values are consistent with the literature.

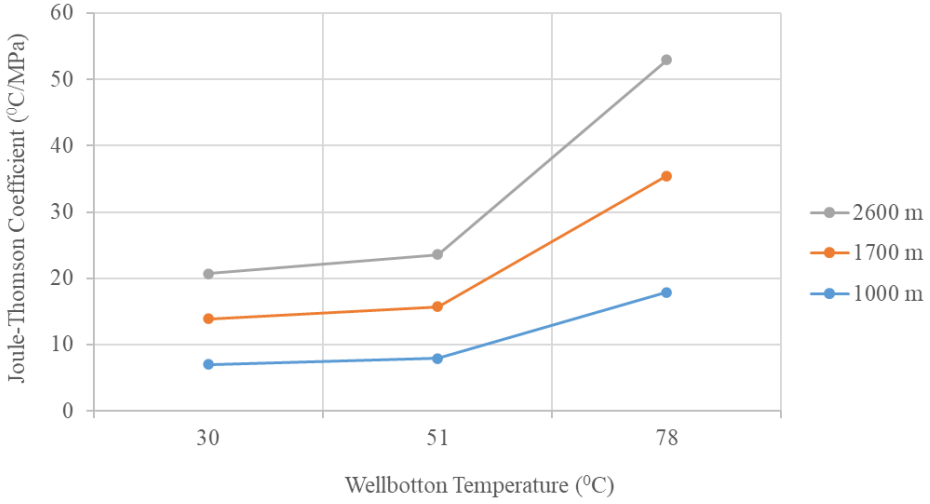

Figure 9. Change in Joule-Thomson Coefficient Depending on Well bottom Temperature.

Carbon dioxide (CO2), initially at atmospheric pressure and a temperature of 5°C at the well bottom, was analysed at various depths. The physical exergy value due to the Joule-Thomson effect (throttling exergy) was calculated as 10.49 at 1000 m depth (3.8 MPa, 30°C), 16.29 at 1700 m depth (4.3 MPa, 51°C), and 25.26 at 2600 m depth (6.1 MPa, 78°C). The throttling exergy associated with CO2 entering the well bottom and exiting the atmosphere was determined to be 581.4 at 1000 m depth (3.8 MPa, 30°C), 527.86 at 1700 m depth (4.3 MPa, 51°C), and 557.5 at 2600 m depth (6.1 MPa, 78°C). The ratio in throttling exergy efficiency, based on the wellhead and well bottom, was calculated as 10.766 at 1000 m depth (3.8 MPa, 30°C), 4.905 at 1700 m depth (4.3 MPa, 51°C), and 3.042 at 2600 m depth (6.1 MPa, 78°C).

IV. CONCLUSIONS

As the well depth and well bottom temperature increase, heat loss through conduction and convection also increases. Depending on the type of rock/soil, well depth, and well bottom temperature, heat loss through conduction was calculated to range from 73.460 to 824.920. Heat loss through convection ranged from 49.542 to 342.940. The total heat loss was determined to be between 123.002 and 1167.860. The difference in heat loss between the well inlet and outlet ranged from 23.918 to 481.980 for conduction and convection.

The Joule-Thomson coefficient decreases as the well depth increases but increases with rising well bottom temperature. Depending on the well depth and temperature, the Joule-Thomson coefficient was found to vary between 6.797 and 17.91.

The change in exergy efficiency due to the Joule-Thomson effect (throttling exergy) was calculated to vary between 3.042 and 10.766, depending on the well depth, pressure, and temperature. Similarly, the throttling exergy was determined to range from 557.5 to 581.4 under varying depth, pressure, and temperature conditions.

Future studies in this field could focus on optimizing heat loss management techniques by incorporating advanced materials and innovative insulation technologies tailored to various rock and soil types. Additionally, research could explore the relationship between well depth (3000 and 4000 m), temperature (80-100 ^{0}C) pressure (7-10 MPa), and the Joule-Thomson coefficient to develop predictive models that enhance geothermal and oil extraction efficiency. As the industry moves toward sustainable practices, integrating renewable energy solutions and minimizing environmental impact will likely become key focus areas.

Authors' Contributions

All authors contributed to the conception and design. Ismail Caner performed conceptualization, funding acquisition, writing review, and editing. Okan Kon conducted conceptualization, methodology, supervision, and writing-original draft. All authors read and approved the final manuscript.

Competing Interests

The authors declare that they have no relevant financial or other interests.

References

[1] Metz, B., Davidson, O., De Coninck, H. C., Loos, M., & Meyer, L. (2005). IPCC special report on carbon dioxide capture and storage. Cambridge: Cambridge University Press.

[2] Rifat US, Çağlar S, Elif K, Türkiye'nin Karbon Yakalama, Kullanma ve Depolama Potansiyeli, Kaynak, Çevre ve İklim Derneği – REC, Mart 2024, Ankara

[3] Olajire, A. A. (2020). Flow assurance issues in deep-water gas well testing and mitigation strategies with respect to gas hydrates deposition in flowlines—A review. Journal of molecular liquids, 318, 114203. https://doi.org/10.1016/j.molliq.2020.114203

[4] Li, Z., Dong, M., Li, S., & Huang, S. (2006). CO2 sequestration in depleted oil and gas reservoirs—caprock characterization and storage capacity. Energy conversion and management, 47(11-12), 1372-1382. https://doi.org/10.1016/j.enconman.2005.08.023

[5] Aminu, M. D., Nabavi, S. A., Rochelle, C. A., & Manovic, V. (2017). A review of developments in carbon dioxide storage. Applied Energy, 208, 1389-1419. https://doi.org/10.1016/j.apenergy.2017.09.015

[6] Liu, X., Falcone, G., & Alimonti, C. (2018). A systematic study of harnessing low-temperature geothermal energy from oil and gas reservoirs. Energy, 142, 346-355. https://doi.org/10.1016/j.energy.2017.10.058

[7] Luo, Y., Xu, G., & Yan, T. (2020). Performance evaluation and optimization design of deep ground source heat pump with non-uniform internal insulation based on analytical solutions. Energy and Buildings, 229, 110495. https://doi.org/10.1016/j.enbuild.2020.110495

[8] Wang, Z., Fan, W., Sun, H., Yao, J., Zhu, G., Zhang, L., & Yang, Y. (2020). Multiscale flow simulation of shale oil considering hydro-thermal process. Applied Thermal Engineering, 177, 115428. https://doi.org/10.1016/j.applthermaleng.2020.115428

[9] Guo, Y., Zhao, J., & Liu, W. V. (2024). Effects of varying heat transfer rates for borehole heat exchangers in layered subsurface with groundwater flow. Applied Thermal Engineering, 247, 123007. https://doi.org/10.1016/j.applthermaleng.2024.123007

[10] Bai, M., Zhang, Z., & Fu, X. (2016). A review on well integrity issues for CO2 geological storage and enhanced gas recovery. Renewable and Sustainable Energy Reviews, 59, 920-926. https://doi.org/10.1016/j.rser.2016.01.043

[11] Amar, M. N., Ghahfarokhi, A. J., & Zeraibi, N. (2020). Predicting thermal conductivity of carbon dioxide using group of data-driven models. Journal of the Taiwan Institute of Chemical Engineers, 113, 165-177. https://doi.org/10.1016/j.jtice.2020.08.001

[12] Liu, Z., Yang, W., Xu, K., Zhang, Q., Yan, L., Li, B., ... & Yang, M. (2023). Research progress of technologies and numerical simulations in exploiting geothermal energy from abandoned wells: a review. Geoenergy Science and Engineering, 224, 211624. https://doi.org/10.1016/j.geoen.2023.211624

[13] Jia, M., Deng, S., Li, X., Jin, W., Yang, Z., & Rao, D. (2023). A numerical simulation study of the micro-mechanism of CO2 flow friction in fracturing pipe string. Gas Science and Engineering, 112, 204941. https://doi.org/10.1016/j.jgsce.2023.204941

[14] Zhou, Y., Liu, Z., & Xing, C. (2022). Application of abandoned wells integrated with renewables. In Utilization of Thermal Potential of Abandoned Wells (pp. 255-273). Academic Press. https://doi.org/10.1016/B978-0-323-90616-6.00013-0

[15] Kengerli, T. S., & Agayeva, N. A. (2024). Influence of connecting a new gas pipeline to the operating gas pipeline on the flow rate of production wells. https://doi.org/10.53404/Sci.Petro.20240100053

[16] Apak, E. C. (2006). A study on heat transfer inside the wellbore during drilling operations. Master's thesis, Middle East Technical University.

[17] Sorgun, M. (2010). Modeling of Newtonian fluids and cuttings transport analysis in high inclination wellbores with pipe rotation.

[18] Ettehadi, A. (2016). Modelling Wellbore Hydraulics through Thermal Rheological Sepiolite Mud Properties. PhD thesis, Graduate School of Science, Engineering and Technology, Istanbul Technical University.

[19] Ahmed, N., Kabir, E., & Islam, M. A. (2024, April). The influence of borehole lengths on a numerical model of a double-tube vertical ground heat exchanger. In IOP Conference Series: Materials Science and Engineering (Vol. 1305, No. 1, p. 012002). IOP Publishing. https://doi.org/10.1088/1757-899X/1305/1/012002

[20] Holloway, S. (2007). Carbon dioxide capture and geological storage. Philosophical Transactions of the Royal Society A: Mathematical, Physical and Engineering Sciences, 365(1853), 1095-1107. https://doi.org/10.1098/rsta.2006.1953

[21] Bachu, S. (2003). Screening and ranking of sedimentary basins for sequestration of CO2 in geological media in response to climate change. Environmental Geology, 44(3), 277-289. https://doi.org/10.1007/s00254-003-0762-9

[22] Bahadori, A., & Vuthaluru, H. B. (2010). Predictive tool for an accurate estimation of carbon dioxide transport properties. International Journal of Greenhouse Gas Control, 4(3), 532-536. https://doi.org/10.1016/j.ijggc.2009.12.007

[23] Vesovic, V., Wakeham, W. A., Olchowy, G. A., Sengers, J. V., Watson, J. T. R., & Millat, J. (1990). The transport properties of carbon dioxide. Journal of physical and chemical reference data, 19(3), 763-808. https://doi.org/10.1063/1.555875

[24] Lim, O.S. Optimization of Gas Transmission Design. 2011. Available online: http://utpedia.utp.edu.my/id/eprint/10565/1/20 11%20-%20Optimizing%20of%20gas%20transmission%20design.pdf (accessed on 22 Jan 2025).

[25] Sagir, M., Mushtaq, M., Tahir, M. S., Tahir, M. B., Ullah, S., Abbas, N., & Pervaiz, M. (2018). CO2 capture, storage, and enhanced oil recovery applications. Encyclopedia of Renewable and Sustainable Materials. Elsevier, 52-58. https://doi.org/10.1016/B978-0-12-803581-8.10360-1

[26] Wu, Z., Xu, J., Wang, X., Chen, K., Li, X., & Zhao, X. (2011). Predicting temperature and pressure in high-temperature–high-pressure gas wells. Petroleum Science and Technology, 29(2), 132-148. https://doi.org/10.1080/10916460903330213

[27] Kurnia, J. C., Shatri, M. S., Putra, Z. A., Zaini, J., Caesarendra, W., & Sasmito, A. P. (2022). Geothermal energy extraction using abandoned oil and gas wells: Techno-economic and policy review. International Journal of Energy Research, 46(1), 28-60. https://doi.org/10.1002/er.6386

[28] Shoghl, S. N., Naderifar, A., Farhadi, F., & Pazuki, G. (2020). Prediction of Joule-Thomson coefficient and inversion curve for natural gas and its components using CFD modeling. Journal of Natural Gas Science and Engineering, 83, 103570. https://doi.org/10.1016/j.jngse.2020.103570

[29] Chevarunotai, N. (2014). Analytical Models for Flowing-Fluid Temperature Distribution in Single-Phase Oil Reservoirs Accounting for Joule-Thomson Effect. PhD thesis.

[30] Islam, R. (2017). Analytical Model for Fluid Temperature Change During Expansion in the Reservoir. PhD thesis.

[31] Ding, L., Yang, Z., Chen, W., & Zhang, Q. (2023). Transient prediction method for flow temperature at wellbore bottom. Applied Thermal Engineering, 234, 121208. https://doi.org/10.1016/j.applthermaleng.2023.121208

[32] Randolph, J. B., Adams, B., Kuehn, T. H., & Saar, M. O. (2012). Wellbore heat transfer in CO2-based geothermal systems. Geothermal Resources Council Transactions, 36, 549-554.
[33] Van Der Meer, B. (2005). Carbon dioxide storage in natural gas reservoir. Oil & gas science and technology, 60(3), 527-536. https://doi.org/10.2516/ogst:2005035
[34] Kon, O. (2004). Termodinamik kısılma ve madde özelliklerine etkisi. Master's thesis, Balıkesir Üniversitesi Fen Bilimleri Enstitüsü.
[35] Kon, O. (2009). Termodinamik kısılma olayında Joule-Thomson katsayısı ve inversiyon eğrileri. Balıkesir Üniversitesi Fen Bilimleri Enstitüsü Dergisi, 11(2), 81-93.
[36] Randolph, J. B., & Saar, M. O. (2011). Combining geothermal energy capture with geologic carbon dioxide sequestration. Geophysical Research Letters, 38(10). https://doi.org/10.1029/2011GL047265
[37] Phillip L. Swagel, Carbon Capture and Storage in the United State, December 2023.
[38] Energy, Technology, & Policy, Carbon Dioxide Enhanced Oil Recovery: A Great Environmental Choice, https://webberenergyblog.wordpress.com/2012/04/01/carbon-dioxide-enhanced-oil-recovery-a-great-environmental-choice/ (access: 12.27.2024)
[39] Huang, Y., Zheng, Q. P., Fan, N., & Aminian, K. (2014). Optimal scheduling for enhanced coal bed methane production through CO2 injection. Applied energy, 113, 1475-1483. http://dx.doi.org/10.1016/j.apenergy.2013.08.074
[40] [40] Samuel, R. J. (2019). Transient flow modelling of carbon dioxide (CO2) injection into depleted gas fields. PhD thesis. University College London.
[41] Gaurina-Međimurec, N., & Pašić, B. (2011). Design and mechanical integrity of CO2 injection wells. Rudarsko-Geolosko-Naftni Zbornik, 23.
[42] CO2 injection well in Mississippi, https://www.usgs.gov/media/images/co2-injection-well-mississippi, April 9, 2010 (access: 12.26.2024)
[43] Witkowski, A., Majkut, M., & Rulik, S. (2014). Analysis of pipeline transportation systems for carbon dioxide sequestration. Archives of thermodynamics, 35(1), 117-140. http://dx.doi.org/10.2478/aoter-2014-0008
[44] Lu, T., Li, Z., Fan, W., & Li, S. (2016). CO2 huff and puff for heavy oil recovery after primary production. Greenhouse Gases: Science and Technology, 6(2), 288-301. https://doi.org/10.1002/ghg.1566
[45] Longe, P. O., Danso, D. K., Gyamfi, G., Tsau, J. S., Alhajeri, M. M., Rasoulzadeh, M., ... & Barati, R. G. (2024). Predicting CO2 and H2 Solubility in Pure Water and Various Aqueous Systems: Implication for CO2–EOR, Carbon Capture and Sequestration, Natural Hydrogen Production and Underground Hydrogen Storage. Energies, 17(22), 5723. https:// doi.org/10.3390/en17225723
[46] Chow, Y. F., Maitland, G. C., & Trusler, J. M. (2016). Interfacial tensions of the (CO2+ N2+ H2O) system at temperatures of (298 to 448) K and pressures up to 40 MPa. The Journal of Chemical Thermodynamics, 93, 392-403.http://dx.doi.org/10.1016/j.jct.2015.08.006
[47] Wang, R., Shi, M., Zhu, K., Yu, J., Ren, W., Yan, G., ... & Gao, S. (2024). Research on the heat transfer model of double U-pipe ground heat exchanger based on in-situ testing. Frontiers in Energy Research, 12, 1442185. https://doi.org/10.3389/fenrg.2024.1442185
[48] Fuchs, S., Balling, N., & Förster, A. (2015). Calculation of thermal conductivity, thermal diffusivity and specific heat capacity of sedimentary rocks using petrophysical well logs. Geophysical Journal International, 203(3), 1977-2000. https://doi.org/10.1093/gji/ggv403
[49] Mobaraki, H. (2024). The Cooling Effect of Joule Thomson on CO2 Storage during Start-Up Period: Integration of Reservoir and Wellbore. PhD thesis, Politecnico di Torino.
[50] Shoghl, S. N., Naderifar, A., Farhadi, F., & Pazuki, G. (2021). Thermodynamic analysis and process optimization of a natural gas liquid recovery unit based on the Joule–Thomson process. Journal of Natural Gas Science and Engineering, 96, 104265. https://doi.org/10.1016/j.jngse.2021.104265
[51] Çengel, Y. A., & Ghajar A.F. (2015). Isı ve Kütle Transferi, Palme Yayınevi.
[52] Kayansayan N., Thermodynamics Principle & Applications, Nobel Akademik Yayıncılık, 2013.
[53] Span, R., & Wagner, W. (1996). A new equation of state for carbon dioxide covering the fluid region from the triple-point temperature to 1100 K at pressures up to 800 MPa. Journal of physical and chemical reference data, 25(6), 1509-1596. https://doi.org/10.1063/1.555991
[54] Menon, E.S. (2005). Gas Pipeline Hydraulics (1st ed.). CRC Press. https://doi.org/10.1201/9781420038224
[55] Luo, Y., & Wang, X. (2010). Exergy analysis on throttle reduction efficiency based on real gas equations. Energy, 35(1), 181-187. https://doi.org/10.1016/j.energy.2009.09.008
[56] Kotas, T. J. (2012). The Exergy Method of Thermal Plant Analysis, 1985. Great Britain by Anchor Brendon Ltd, Tiptree, Essex.
[57] Li, J., Chen, Y., Ma, Y. B., Kwon, J., & Xu, H. (2023). Ji-Chao Li A study on the Joule-Thomson effect of during filling hydrogen in high pressure tank, Case Studies in Thermal Engineering, 41, 102678. https://doi.org/10.1016/j.csite.2022.102678

[58] Erdoğan, M., & Acar, M. Ş. (2024). Thermodynamic analysis of a tunnel biscuit oven and heat recovery system. *WAPRIME*, *1*(1), 1-15.

[59] Ünal, E. K. (2024). Analytical and numerical investigation of viscous heating in parallel-plate Couette flow. WAPRIME, 1(1), 57-69.